Monitoring impedance changes associated with motility and mitosis of a single cell†

Lamya Ghenim,*[a] Hirokazu Kaji,[bc] Yu Hoshino,[b] Takeshi Ishibashi,[b] Vincent Haguet,[a] Xavier Gidrol[a] and Matsuhiko Nishizawa[bc]

Received 10th March 2010, Accepted 11th June 2010
DOI: 10.1039/c004115g

We present a device enabling impedance measurements that probe the motility and mitosis of a single adherent cell in a controlled way. The micrometre-sized electrodes are designed for adhesion of an isolated cell and enhanced sensitivity to cell motion. The electrode surface is switched electrochemically to favour cell adhesion, and single cells are attracted to the electrode using positive dielectrophoresis. Periods of linear variation in impedance with time correspond to the motility of a single cell adherent to the surface estimated at 0.6 μm h^{-1}. In the course of our study we observed the impedance changes associated with mitosis of a single cell. Electrical measurements, carried out concomitantly with optical observations, revealed three phases, prophase, metaphase and anaphase in the time variation of the impedance during cell division. Maximal impedance was observed at metaphase with a 20% increase of the impedance. We argue that at mitosis, the changes detected were due to the charge density distribution at the cell surface. Our data demonstrate subtle electrical changes associated with cell motility and for the first time with division at the single-cell level. We speculate that this could open up new avenues for characterizing healthy and pathological cells.

1 Introduction

Both cell–surface interactions and cell locomotion are extremely important in biology, as these properties are central to the processes of cell differentiation and organ development.[1] In medicine, they play a major role in the metastatic behavior of cells from malignant solid tumors.[2] In general, mammalian cell migration has been studied optically by forming wound edges in a single layer of cultured cells and measuring how rapidly cells repopulate the wound edges.[3] While such optical characterization is considered the standard, Giaever and Keese, pioneered the use of impedance measurements to study biological processes in cells[4–8] and organisms. In particular, they introduced the idea of measuring cell motility electrically.[9] They demonstrated that the impedance traces of metastatic cells were very different from those of normal cells. Recently, Wang *et al.*[10] used self-assembled monolayers (SAMs) on gold electrodes to inhibit cell adherence and thus mimic wounds in a cell monolayer. They induced cell migration by applying a DC electrical signal on the gold electrodes in order to desorb the SAMs and measured the process of cell migration by real-time impedance-sensing. In these studies, the dimensions of the electrodes were such that the average movement of hundreds of cells was measured. An alteration in the impedance of an entire cell population is interesting, but it would be even more valuable to extend impedance measurements down to the level of a single cell, which could exhibit specific electrical properties. Parameters that are measured as averages of large populations can be misleading. For instance an apparently linear response to a signal could in fact reflect an increasing number of cells in the population that have switched from "off" to "on" rather than an incremental increase in response by all the cells.[11] The ability to study single cells will permit a better understanding of cellular heterogeneity[12] which is significant in growth, division and infection. Cells, even genetically identical, in an *in vitro* population, are not homogeneous entities. A growing number of studies on enzyme activity, gene expression or response to signaling indicate that there is substantial cell-to-cell variability. It has been shown recently that differences in the levels or states of proteins regulating receptor-mediated apoptosis are the primary causes of cell-to-cell variability in the timing and probability of death in human cell lines.[13] This has an impact for understanding "fractional killing" of tumor cells after exposure to chemotherapy. Traditionally, this was thought to reflect differences in genotype, cell cycle state or the involvement of cancer stem cells. Other work has shown that the population context determines cell-to-cell variability in endocytosis and virus infection.[14] Cell-to-cell variation has also been demonstrated in gene expression in ageing mouse heart.[15] As a consequence, methods that can be used on single cells are needed. Cellular impedance biosensors offer an alternative to conventional analytical techniques with potential advantages of high speed, accuracy, sensitivity, non-invasiveness, and easiness in direct computer analysis. The immediate aim of our work is to develop new tools for analyzing the fundamental biology of single adhesive cells and pave the way to understanding how the measured heterogeneity contributes to cellular function.

Lind *et al.*[16] observed a qualitative relationship between the impedance change and the motility of a single cultured BHK

[a]*CEA, iRTSV, Laboratoire Biopuces, 17 Rue des Martyrs, 38054 Grenoble, France. E-mail: lamya.ghenim@cea.fr; Fax: +33 438785917; Tel: +33 438789187*
[b]*Department of Bioengineering and Robotics, Graduate School of Engineering, Tohoku University, 6-6-01 Aoba, Sendai, 980-8579, Japan*
[c]*JST, CREST, Sanbancho, Chiyoda-ku, Tokyo, 102-0075, Japan*
† Electronic supplementary information (ESI) available: Fig. S1 and S2; Movie S1–S3. See DOI: 10.1039/c004115g

fibroblast on an untreated sensing electrode the same size as the cell. In those experiments, the cells were seeded randomly on the sensing electrode. In the present study, we also reduced the scale of the electrode so as to be able to probe individual cells. In addition, the electrode surface was engineered to favor cell adhesion by an electrochemical-based surface modification,[17] and we were able to attract a single cell toward the edge of this electrode, in a controlled way, by positive dielectrophoresis (DEP).[18] Our measurements were facilitated by the fact that the changes of impedance with electrodes comparable to cell size were much larger than those (a few percent) found by Giaever and Keese,[9] whose electrodes were 1 cm and 100 μm long. Consequently, we did not need the amplification provided by low-noise voltage source instrumentation.

We report then a novel device enabling impedance measurements, without signal amplification, that probes the motility and mitosis of a single adherent cell attracted to the electrode by positive dielectrophoresis. Previously, Halvorsud *et al.*[19] have monitored electrically the contraction rhythm in plasmodia of *Physarum polycephalum* and have shown features of the impedance trace that correspond to mitosis, by comparing with fluorescence methods and aceto-orcein coloring techniques. They did not, however, provide the detailed signature of the different phases of mitosis. Here, we observed, for the first time, subtle impedance changes associated to the different phases of mitosis in mammalian cells. This may open up new avenues for characterizing healthy and pathological cells.

2 Materials and methods

2.1 Fabrication of electrodes

Our system was designed as a ring-shaped counter platinum (Pt) electrode 1 mm in diameter, which encircles a 20 μm diameter round sensing electrode (Fig. 1A). The gap between electrodes was 100 μm. Instead of using rectangular planar electrodes,[9] we used radially symmetric concentric planar electrodes, so that the sensing electrode can trap and detect a cell arriving from any direction. The dimensions were chosen to match HeLa cells. Due to the high asymmetry of the electrode areas, the total impedance was dominated by the sensing electrode. In the frequency range 1–100 kHz its impedance is, in fact, that of the interface between the ionic buffer and the sensing electrode[9] (see ESI† Fig. S1),

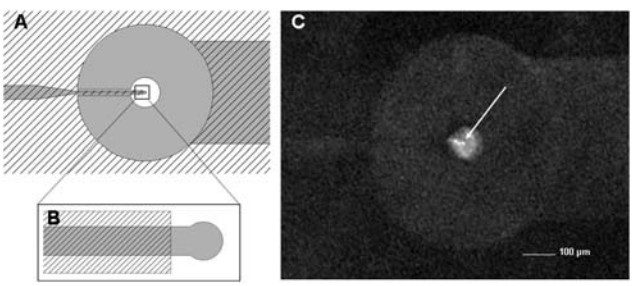

Fig. 1 (A) Schematic representation of the electrodes. The electrodes are gray and the SU-8 photoresist is hatched. (B) Enlarged version of the sensing electrode. (C) Fluorescence image of the system after electrochemical treatment and fibronectin-Cy3 deposition. The arrow indicates the sensing electrode.

precisely where the cells adhere. At these frequencies, the cells can be considered insulating particles.[20] The impedance changes because the current is forced to flow around the cells that cover part of the electrode.[16] Cell motility can lead to significant variations in the impedance, which is roughly inversely proportional to the difference of comparable areas: that of the sensing electrode and that area blocked by cells in contact with the electrode. The 100 nm thick electrodes were patterned on a glass plate by lift-off of a sputter-deposited Pt/Ti film. Then a negative photosensitive photoresist (SU-8) was spin-coated and insulated to form an 8 μm thick insulating layer covering the whole chip with the exception of the sensing and counter electrode, which are thus exposed. Finally, a silicone chamber (1.1 × 0.7 × 1 cm) was bonded at the center of the substrate to form a large chamber for cell culture and migration assays.

2.2 Selective adsorption of fibronectin on the sensing electrode

Electrochemical-based surface patterning was used to induce local cell adhesion on the smaller electrode.[17] The patterning was carried out in a two-electrode configuration with an Ag/AgCl (saturated KCl) counter electrode immersed in the solution and the smaller sensing electrode as the working electrode. Solutions of polyethyleneimine (PEI, 5 mg ml^{-1} in deionized water (DI)) and heparin (2 mg ml^{-1} in DI) were first poured into the chamber to form an anti-biofouling layer. A pulse of 1.7 V was applied for 2 s between the two electrodes of the electrochemical cell in phosphate buffered saline (PBS) solution containing 25 mM KBr. This procedure resulted in electrochemical oxidation of Br^- to Br_2 (subsequently HBrO) at the electrode, causing the rapid detachment of the anti-biofouling layer and, as a result, uncoated spots. These spots were filled with fibronectin, a protein with cell adhesive properties. Fig. 1C shows the patterns of the highly fluorescent labeled fibronectin (fibronectin-Cy3) on the electrodes. The background is due to SU-8 parasitic fluorescence. The fibronectin adsorbs on and near the sensing electrode in a circular fashion, corresponding to an expansion of the HBrO diffusion layer. The size of the fibronectin pattern can be controlled by the electrolysis period of HBrO.

2.3 AC electrical measurements

AC electrical measurements were carried out in PBS on bare electrodes (conductivity $\sigma = 16.2$ mS cm^{-1}) or in serum-free culture medium (GIT medium, Nihon Pharmaceutical Co., Tokyo, Japan) ($\sigma = 13.4$ mS cm^{-1}) on electrodes with cells in the two-probe configuration of an electrochemical analyzer (Model 600S, BAS). The sensing electrode was chosen as the working electrode and the larger electrode as the counter. A voltage of 10 mV was applied across the electrodes. Measurements (see ESI† Fig. S1 and S2) in the range of $f = 1$–100 kHz show that the total impedance has the behavior $Z = K(jf)^{-\alpha}$ with K a constant and the value of α varying from electrode to electrode, but always remaining less than 1. This is consistent with generalizations of the Warburg model[21] of an electrode–electrolyte interface. A double layer of charges at the interface behaves like a parallel plate capacitor. Diffusion of ions to the interface from the bulk of the electrolyte gives rise to the power law behavior. For the original Warburg model of a perfect interface α is 0.5,

as observed experimentally in perfectly planar interfaces. Such an empirical power law, but with a general exponent, has been shown to apply for a variety of less perfect solid–electrolyte interfaces where the departure of α from 0.5 reflects surface roughness in particular. In the full electrical circuit model (as in the ESI†) the electrode–electrolyte interface impedance is in parallel with the charge transfer resistance R_b due to charge leakage across the double layer induced by electrochemical reactions (DC behavior), and in series with the solution resistance R_s. At 4 kHz the contribution of solution resistance is small (see ESI† Fig. S1 and S2): the total resistance is dominated by the interface impedance (ionic buffer–Pt sensing electrode). We worked at 2.5 kHz and 4 kHz to maximize sensitivity while avoiding diverging impedances at very low f.

2.4 Positive dielectrophoresis

Initially, we used positive DEP[18] to attract a very small number of cells to the edge of the sensing electrode after fibronectin pattern formation. A small concentration of cells in the chamber (10^3 cells ml^{-1}) was used. To enhance cell polarization compared to the medium (positive DEP), we used an iso-osmotic low-conductivity buffer (8.5% sucrose and 0.3% glucose in DI, $\sigma = 2$ μS cm^{-1}) and applied an AC voltage of 5 V at 1 MHz across the electrodes with a function generator (model FG-163, NF Corporation, Japan).[22] The cells were attracted towards the region of strongest electric field, *i.e.* the edge of the smaller electrode. After 5 min of DEP, cells adhered efficiently and the voltage was turned down. We successfully attracted a single or a few cells to the edge of the sensing electrode within a few minutes (see Movie S1†). Consistent with previous results,[22,23] we did not observe any effect of DEP on cell viability. We note that after this phase of DEP to place the cell on the electrode, the electrical measurements were carried at a much lower frequency (kHz), as detailed above.

2.5 Cell culture

HeLa cells were cultured in a serum-free culture medium (GIT medium, Nihon Pharmaceutical Co., Tokyo, Japan), which contains proteins and nutrients for cell maintenance, at 37 °C under a 5% CO_2 atmosphere. A subconfluent cell monolayer was dissociated with a 0.25% trypsin solution, suspended in medium and seeded onto a patterned substrate. To limit cell proliferation during the motility experiments, cells were treated with 10 μM thymidine for 24 h before, and during, the assay.[24] The chamber was rinsed with medium alone to eliminate non-adherent cells before incubation; the end of the rinsing process defines the time origin $t = 0$ in our data.

2.6 Microscopy

Time lapse images of the cells were acquired using an inverted microscope (TE300, Nikon, Tokyo, Japan) equipped with an on-stage incubation chamber (INUG2-ONICS, Tokai Hit Co., Ltd., Shizuoka, Japan) that kept the cells at 37 °C under a 5% CO_2 atmosphere. Optical images, recorded using a digital CCD camera (Luca, Andor Technology, South Windsor, CT, USA) every ten minutes, were analyzed using MetaMorph software (Molecular Devices, Sunnyvale, CA, USA).

3 Results and discussion

3.1 Single-cell motility

Fig. 2 shows the impedance changes for one typical experiment where the motion of a single cell dominated, normalized to the impedance of the surface covered with fibronectin alone, *i.e.* without cells. The data of Fig. 2 were taken every minute and smoothed by 10-point adjacent averaging. We simultaneously followed the cells optically.

Initially, two cells were attracted to the edge of the electrode, while there were almost no cells left on the glass. The impedance did not always increase monotonically and had a history specific to each experiment. Snapshots of cells or the full movie (see Movie S2†) exquisitely show how motility or key cellular events affected the time-course of impedance. Initially, (A) two cells attached and spread on the electrode, producing a large increase in impedance. The time scale of spreading was known to be a fraction of an hour. From (A) to (B) the two cells contributed to the signal while moving on the electrode. Between (B) and (C) the upper cell moved gradually away from the electrode, which was reflected by a decrease in impedance; at the same time, the lower cell apparently remained stationary. Between (C) and (D) the upper cell separated completely from the electrode and the lower cell moved towards the center of the sensing electrode, thus no longer contributing to the impedance. As a result, the impedance should drop to the value of the fibronectin-coated electrode, as observed. From (D) to (E) and (F) the upper cell re-attached and progressively covered a considerable part of the electrode. This final period, in which one cell moved back onto the electrode, provided a simple estimate of the motility. Between (D) and (F), the impedance of the electrode partially covered by the upper cell varied about 20% during a period of 16 h. The change was triggered by the motility of a single cell, and, as demonstrated from the images, it moved a distance of approximately the radius of the electrode (10 μm). We can thus give a rough estimate of the individual motility of a cell, as 10 μm over

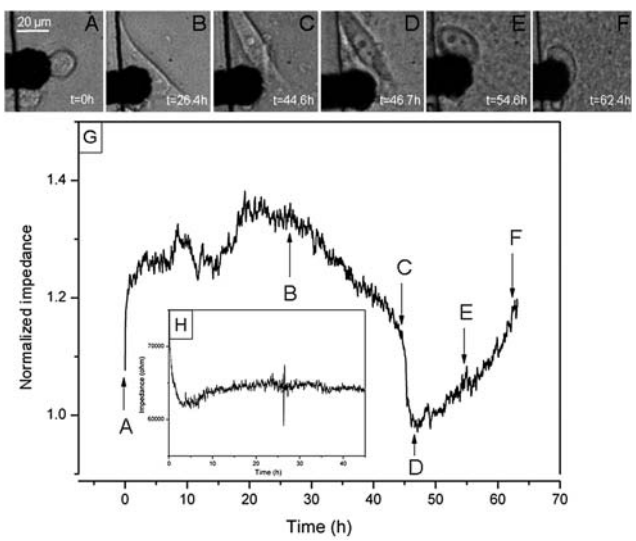

Fig. 2 Normalized impedance trace (G) for two cells attracted by positive DEP, correlated with snapshots (A–F) of cell positions at key times. Inset (H): Impedance of a dead cell on the electrode.

16 h $\approx$ 0.6 μm h^{-1}. This should be compared to the 5 μm h^{-1} average cell motility estimate of Wang *et al.*[10] We emphasize that in their measurements, there were a large number of HeLa cells attached to the electrodes, while our measurements reflected the motility of a single, isolated cell without the influence of cell–cell interactions. A cell does not actually move in one direction but may follow a random path. If we had only the resistance curve, we would have had to know that the 20% change in resistance corresponded to the maximal change in coverage by a single cell. Once this calibration is established, however, for the electrode design and the cell size, impedance measurements alone should suffice to estimate cell motility. As a control experiment, the impedance changes in the presence of a dead cell on the electrode were monitored (see Fig. 2H inset). The optical validation showed no motion of this cell, and, as expected, the impedance trace remained completely flat over the entire experiment after an initial period in which the temperature stabilizes.

3.2 Detecting single-cell mitosis on an electrode

In the course of our study we fortuitously observed the impedance changes associated with the mitosis of a single cell. Electrical measurements were validated concomitantly by optical observations. One cell was attracted onto the electrode *via* positive DEP and then electrically and visually monitored for just over 2 days (see Fig. 3L Inset). The data of Fig. 3 were taken every minute but no averaging was required.

The cell did not move much during the first 20 h, corresponding to the relatively flat impedance, but then the complexity of the impedance data increased. Most interesting is the peak around $t = 24$ h, which corresponds to the mitosis of this cell, as shown in Fig. 3 and Movie S3.† By expanding the time scale around this peak we observed three distinct phases in the variation of the impedance (Fig. 3). First, there was a slow increase (snapshots A to F), which lasted about 50 min and, as shown by the movie snapshots, corresponds to the time when the cell switched from a flattened and extended shape to assume a spherical morphology. We identify this as the prophase. Second, the impedance increased sharply over a short period of time (10 min) to reach a maximum at snapshot G, in which one can see condensation of the chromosomes in the equatorial plate. This corresponds to metaphase, which usually represents ~1% of the duration of the cell cycle but is slightly longer in HeLa cells. Third, the impedance decreased between snapshots G and K. This last period corresponds to anaphase, telophase and cytokinesis. In snapshot H, we observed the separation of sister chromatids, and later, in snapshot I, we observed the cleavage furrow and the membrane formation between the two daughter cells, which finalized mitosis (snapshots J and K). During this last phase, only one daughter cell was left on the sensing electrode. After snapshot K, the impedance decreased as this cell gradually left the electrode. The measured time constants for prophase, metaphase, and anaphase/telophase/cytokinesis perfectly matched the time constants optically observed during mitosis of HeLa cells.[25]

To our surprise, metaphase was associated with the maximal impedance observed during mitosis. Indeed, as the cell becomes spherical, one would expect a reduced contact with the planar electrode, leading to lower impedance following the arguments given above. This would be consistent with a previous study that showed that the total cell surface area decreases during cell rounding and reaches a minimum at metaphase.[26,27] During the transition from a flat cell at interphase (A) to a spherical cell at metaphase (G), the field lines between the two planar electrodes

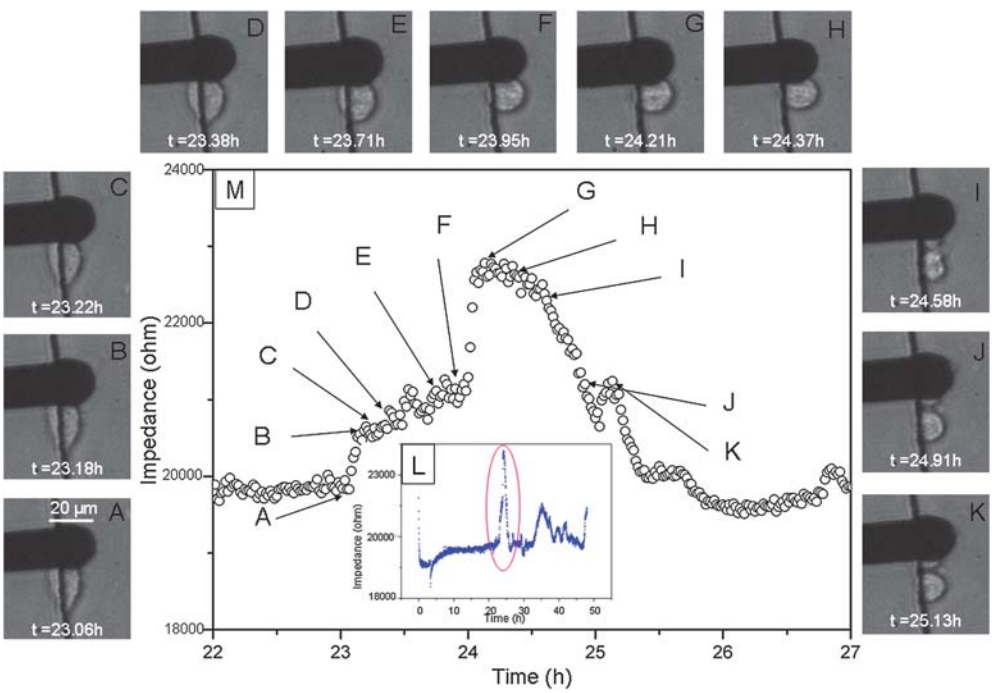

Fig. 3 Impedance trace (M) during the mitosis of one single cell, correlated with snapshots (A–K) of cell positions at key times. We observe prophase (A–F), metaphase (G) and anaphase (H). Insert (L): the trace over the full 2 days of the experiment.

should be affected, but a strong increase in impedance seemed unlikely. The resolution of this issue lies in the fact that we were also measuring the interface impedance between the cell and the electrode surrounded by the buffer solution. The impedance depends on the interface capacitance, as discussed in the ESI.† Between prophase and metaphase the densities of microtubules change, as does the distribution of chromosomes. Some authors[28,29] have already shown that there is a sharp increase in the electrophoretic mobility of HeLa cells during mitosis. The increased mobility, measured on freely flowing cells subjected to high voltage, is due to an enhancement of net negative charge density at the cell surface. The most likely interpretation for the impedance maximum we observed at metaphase is that we are detecting changes in surface charge density at the cell surface, although we cannot yet rule out contributions from changes in cell morphology and orientation.

Note that the electrophoretic mobility gave a single maximum[29] without the substructures we observed in the impedance trace. We believe our method of measurement enables the monitoring of prophase, metaphase and anaphase/telophase of an individual cell. In the future, observations of mitosis can be optimized by synchronizing the cell cycles.

4 Conclusions

By combining electrochemical-based surface modification and positive DEP with micrometric electrodes, we have constructed a sensitive tool to measure electrically the motility of one single cell without any signal amplification. The signal is very sensitive to the position of the cell relative to the edge of the sensing electrode and therefore depends on the specific trajectory of the cell. In the future the device can be improved by incorporating transparent electrodes[30] in order to better correlate optical observations. Apart from changes due to cell motility, our device enables the monitoring of changes associated with mitosis at the single-cell level and as a consequence should enable direct comparison between cells in different physiological states. For instance, dysfunction of the G2/M checkpoint, which prevents entry into mitosis, and plays a major role on genomic stability and cancer risk. We speculate that monitoring the impedance changes associated with the cell cycle and mitosis of a single cancerous or healthy cell could help detect differences between the two cell types that were not observable before.

Acknowledgements

L.G. thanks the bioMEMS group of Department of Bioengineering and Robotics, Tohoku University for hospitality, and H. Nojiri, IMR, Tohoku University for the loan of electronic equipment. We thank P. Pham for help with electrode design, P. Obeïd, S. Porte, B. Fouqué, D. Skouffias, M. Théry, D. Bicout and E. Kats for discussions. The project was funded in part by a Core Research for Evolutional Science and Technology grant from the Japan Science and Technology Agency.

References

1 A. Huttenlocher, R. R. Sandborg and A. F. Horwitz, *Curr. Opin. Cell Biol.*, 1995, **7**, 697.
2 P. Friedl and K. Wolf, *Nat. Rev. Cancer*, 2003, **3**, 362.
3 A. Q. Cai, K. A. Landman and B. D. Hughes, *J. Theor. Biol.*, 2007, **245**, 576.
4 P. Mitra, C. R. Keese and I. Giaever, *Biotechniques*, 1991, **11**, 504.
5 J. Wegener, C. R. Keese and I. Giaever, *Exp. Cell Res.*, 2000, **259**, 158.
6 C. R. Keese, K. Bhawe, J. Wegener and I. Giaever, *Biotechniques*, 2002, **33**, 842.
7 C. R. Keese, J. Wegener, S. R. Walker and I. Giaever, *Proc. Natl. Acad. Sci. U. S. A.*, 2004, **101**, 1554.
8 B. F. De Blasio, M. Laane, T. Walmann and I. Giaever, *Biotechniques*, 2004, **36**, 650.
9 I. Giaever and C. R. Keese, *IEEE Trans. Biomed. Eng.*, 1986, **33**, 242.
10 L. Wang, J. Zhu, C. Deng, W. Xing and J. Cheng, *Lab Chip*, 2008, **8**, 872.
11 M. E. Lidstrom and D. R. Meldrum, *Nat. Rev. Microbiol.*, 2003, **1**, 158.
12 N. de Souza, *Nat. Methods*, 2010, **7**, 35.
13 S. L. Spencer, S. Gaudet, J. G. Albeck, J. M. Burke and P. K. Sorger, *Nature*, 2009, **459**, 428.
14 B. Snijder, R. Sacher, P. Ramo, E. Damm, P. Liberali and L. Pelkmans, *Nature*, 2009, **461**, 520.
15 R. Bahar, C. H. Hartmann, K. A. Rodriguez, A. D. Denny, R. A. Busuttil, M. E. T. Dolle, R. B. Calder, G. B. Chisholm, B. H. Pollock, C. A. Klein and J. Vijg, *Nature*, 2006, **441**, 1011.
16 R. Lind, P. Connolly, C. D. W. Wilkinson, L. J. Breckenridge and J. A. T. Dow, *Biosens. Bioelectron.*, 1991, **6**, 359.
17 H. Kaji, M. Kanada, D. Oyamatsu, T. Matsue and M. Nishizawa, *Langmuir*, 2004, **20**, 16.
18 C. T. Ho, R. Z. Lin, W. Y. Chang, H. Y. Chang and C. H. Liu, *Lab Chip*, 2006, **6**, 724.
19 R. Halvorsrud, I. Giaever and M. M. Laane, *Protoplasma*, 1995, **188**, 12.
20 S. Gawad, L. Schild and P. Renaud, *Lab Chip*, 2001, **1**, 76.
21 J. Chang, J. Park, Y. K. Pak and J. J. Pak, *3rd Int IEEE EMBS Conf. on Neural Engin., Hawaii, USA*, 2007, 572–574.
22 H. Kaji, M. Hashimoto, S. Sekine, T. Kawashima and M. Nishizawa, *Electrochemistry*, 2008, **76**, 555.
23 M. Hashimoto, H. Kaji and M. Nishizawa, *Biosens. Bioelectron.*, 2009, **24**, 2892.
24 M. L. Whitfield, L. Zheng, A. Baldwin, T. Ohta, M. M. Hurt and W. F. Marzluff, *Mol. Cell. Biol.*, 2000, **20**, 4188.
25 X. Rao, Y. Zhang, Q. Yi, H. Hou, B. Xu, L. Chu, Y. Huang, W. Zhang, M. Fenech and Q. Shi, *Mutat. Res., Fundam. Mol. Mech. Mutagen.*, 2008, **646**, 41.
26 E. Boucrot and T. Kirchhausen, *Proc. Natl. Acad. Sci. U. S. A.*, 2007, **104**, 7939.
27 E. Boucrot and T. Kirchhausen, *PLoS One*, 2008, **3**, e1477.
28 T. P. Brent and J. A. Forrester, *Nature*, 1967, **215**, 92.
29 H. Tsunoo, T. Yamada and K. Aso, *Bull. Tokyo Med. Dent. Univ.*, 1977, **24**, 155.
30 M. Bonnauron, S. Saada, C. Mer, C. Gesset, O. A. Williams, L. Rousseau, E. Scorsone, P. Mailley, M. Nesladek, J.-C. Arnault and P. Bergonzo, *Phys. Status Solidi A*, 2008, **205**, 2126.

